

Natural iron ligands promote a metal-based oxidation mechanism for the Fenton reaction in water environments

Original

Natural iron ligands promote a metal-based oxidation mechanism for the Fenton reaction in water environments / Farinelli, G.; Minella, M.; Pazzi, M.; Giannakis, S.; Pulgarin, C.; Vione, D.; Tiraferri, A.. - In: JOURNAL OF HAZARDOUS MATERIALS. - ISSN 0304-3894. - 393:(2020), p. 122413. [10.1016/j.jhazmat.2020.122413]

Availability:

This version is available at: 11583/2834172 since: 2020-06-09T17:02:21Z

Publisher:

Elsevier B.V.

Published

DOI:10.1016/j.jhazmat.2020.122413

Terms of use:

This article is made available under terms and conditions as specified in the corresponding bibliographic description in the repository

Publisher copyright

(Article begins on next page)

1 **Natural Iron Ligands Promote a Metal-Based Oxidation**

2 **Mechanism for the Fenton Reaction in Water Environments**

3 Giulio Farinelli,[†] Marco Minella,[‡] Marco Pazzi,[‡] Stefanos Giannakis,[§] Cesar

4 Pulgarin,^{||} Davide Vione,^{*,‡} Alberto Tiraferri^{*,†}

5 [†]Department of Environment, Land and Infrastructure Engineering (DIATI), Politecnico di
6 Torino, Corso Duca degli Abruzzi 24, 10129, Turin, Italy

7 [‡]Department of Chemistry, University of Turin, Via Pietro Giuria 7, 10125 Turin, Italy

8 [§]Universidad Politécnica de Madrid, E.T.S. Ingenieros de Caminos, Canales y Puertos,
9 Departamento de Ingeniería Civil: Hidráulica, Energía y Medio Ambiente, Unidad docente
10 Ingeniería Sanitaria, c/ Profesor Aranguren, s/n, ES-28040 Madrid, España

11 ^{||}SB, ISIC, Group of Advanced Oxidation Processes, Ecole Polytechnique Fédérale de
12 Lausanne (EPFL), Station 6, 1015 Lausanne, Switzerland

13
14
15
16 Corresponding Authors

17 Prof. Alberto Tiraferri. E-mail: alberto.tiraferri@polito.it

18 Prof. Davide Vione. E-mail: davide.vione@unito.it

19

20 **Abstract**

21 The Fenton reaction is an effective advanced oxidation process occurring in nature and
22 applied in engineering processes toward the degradation of harmful substances, including
23 contaminants of emerging concern. The traditional Fenton application can be remarkably
24 improved by using iron complexes with organic ligands, which allow for the degradation of
25 contaminants at near-neutral pH and for the reduction of sludge production. This work
26 discusses the mechanisms involved both in the classic Fenton process and in the presence of
27 ligands that coordinate iron. Cyclohexane was selected as mechanistic probe, by following
28 the formation of the relevant products, namely, cyclohexanol (A) and cyclohexanone (K). As
29 expected, the classic Fenton process was associated with an A/K ratio of approximately 1,
30 evidence of a dominant free radical behavior. Significantly, the presence of widely common
31 natural and synthetic carboxyl ligands selectively produced mostly the alcoholic species in
32 the first oxidation step. A ferryl-based mechanism was thus preferred when iron complexes
33 were formed. Common iron ligands are here proven to direct the reaction pathway towards a
34 selective metal-based catalysis. Such a system may be more easily engineered than a free
35 radical-based one to safely remove hazardous contaminants from water and minimize the
36 production of harmful intermediates.

37

38

39

40 **Keywords:** advanced oxidation; Fenton mechanism; iron ligands; free radical mechanism;
41 metal-based catalysis.

42

43 **Highlights**

- 44 • Systematic work investigating the Fenton mechanism in the presence of ligands
- 45 • The presence of ligands promotes metal-based catalysis
- 46 • The oxidation mechanism depends on the concentration of the iron ligand
- 47 • Different Fenton mechanisms occur by varying the pH
- 48 • A ferryl species is reasonably involved in the oxidation pathway with ligands

49

50 1. INTRODUCTION

51 The Fenton reaction has been known since over a century (Fenton 1894; Giannakis 2019) and
52 represents an effective advanced oxidation process to remove many recalcitrant pollutants
53 (Barbeni et al. 1987; Lipczynskakochany 1991; Maillard et al. 1992; Zhang et al. 2006; Liu et
54 al. 2018; Ricceri et al. 2019). Nevertheless, this process has some major drawbacks when
55 applied to contaminated waters, including the need to operate under acidic conditions, the
56 formation of slurries of precipitated iron in the final basification step, and the competition of
57 pollutants with other aqueous species, e.g., carbonate and dissolved organic matter, in the
58 reaction with non-selective free radicals (Pignatello et al. 1999; Vione et al. 2014). A possible
59 solution to tackle these limitations is the use of iron ligands, in analogy with the biological
60 oxidations catalyzed by iron complexes, e.g., Cytochrome P450 (Cyt P450) or Taurine
61 Dioxygenase (TauD) (Hohenberger et al. 2012). The use of similar iron(II) complexes as
62 engineered catalysts is a promising variation of the traditional Fenton process, because it
63 permits the degradation of persistent contaminants at near-neutral pH, while reducing the
64 sludge production by keeping iron in solution (dos Santos et al. 2011; Song et al. 2015;
65 Giannakis et al. 2016; Clarizia et al. 2017; Messele et al. 2019; Das et al. 2020; Pan et al.
66 2020). Moreover, the use of an iron ligand can promote a more selective oxidative action,
67 which increases the efficiency of the treatment and allows control over by-product formation.
68 Such improvements in the selectivity of the reaction depend on the reaction mechanism, more
69 specifically on the active species, but little is known regarding the reaction pathway in these
70 systems. The reaction mechanism is widely debated both for the classic Fenton process and
71 for the modified Fenton process involving the chelation of iron (Barbusinski 2009; Zhang and
72 Zhou 2019). In this work, we evaluate and discuss the application of a simple method to
73 investigate the reaction pathway when iron ligands are present in water.

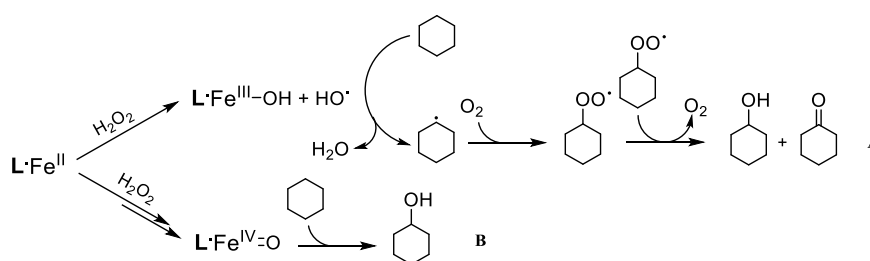
74 The classic description of the traditional Fenton process is based on the first reaction of the
75 Haber-Weiss mechanism proposal (eq. 1) (Haber and Weiss 1932):



77 More recent investigations also proposed a mechanism that includes the formation of a
78 transient species where iron has a formal redox state of IV (Goldstein et al. 1993; Bossmann
79 et al. 1998). The presence of other superoxidized iron species (not only $\text{Fe}^{\text{IV}}_{(\text{aq})}$, but also
80 $\text{Fe}^{\text{V}}_{(\text{aq})}$ and $\text{Fe}^{\text{VI}}_{(\text{aq})}$) has been additionally proven (Wink et al. 1994). However, the reactivity,
81 role, and the stability of such species is only partially known. Essential contributions were
82 provided in the works by Bossmann et al. (1998) and Pignatello et al. (1999), who
83 highlighted the different reactivity of ferryl and hydroxyl radicals and provided evidence of
84 the concurrent presence of different reactive species. More recently, Minero and co-workers
85 corroborated that $\bullet\text{OH}$ (60% yield) and other species (e.g., FeO^{2+}) (40% yield) are formed
86 simultaneously (Minero et al. 2013). As mentioned above, the oxidation mechanism is amply
87 debated also when the system comprises iron complexes, e.g., in the presence of iron ligands.
88 Rush and Koppenol investigated a variety of chelated iron complexes, concluding that a
89 metal-oxo species was generated in neutral solutions, while $\bullet\text{OH}$ species dominated the
90 process in acidic solutions of non-chelated iron (Rush and Koppenol 1988). Sutton et al.
91 (1987) reached a different conclusion, proposing that free iron generates a metal-oxo species
92 as the primary oxidant while $\bullet\text{OH}$ is dominant when chelated iron is present. A reasonable
93 rationalization of this apparent discrepancy is that metal-oxo species and $\bullet\text{OH}$ can both be
94 generated concurrently in Fenton systems. Indeed, Yamazaki and Piette (1990) suggested that
95 more than one type of oxidizing intermediate is present, and that the stoichiometry
96 $\bullet\text{OH}:\text{Fe(II)}$ is also a function of the nature of the prevailing iron chelators. Different chelating
97 agents for Fe(II) have been reported to promote the formation of oxoiron (ferryl) species in

98 addition to, or instead of, $\cdot\text{OH}$, thus accelerating (e.g., with fulvic acid (Southworth and
99 Voelker 2003), oxalate (Park et al. 1997), and EDTA (Rush and Koppenol 1986)) or
100 suppressing (e.g., with phosphates) the Fenton reaction (Iwahashi et al. 1990).

101 Because the direct experimental observation of the key intermediates involved in the
102 oxidation pathways is challenging, indirect probes were developed (Klopstra et al. 2004;
103 England et al. 2008; Oloo and Que 2013; Dong et al. 2018). Cyclohexane (Cy) was used in
104 previous studies as an advantageous tool to discriminate between the different pathways of
105 the Fenton reaction in organic solvents, by following the selective production of two
106 products, namely cyclohexanol and cyclohexanone in different ratios (Oloo and Que 2013).
107 Reactions initiated by hydroxyl radicals produce long-lived alkyl radical intermediates. These
108 intermediates may react with dissolved molecular oxygen at diffusion-controlled rates to
109 produce alkylperoxyl radicals, whose subsequent reaction is a Russell-type termination that
110 gives equimolar quantities of alcohol (A) and ketone (K) (**Scheme 1a**) (Russell 1957;
111 Meslennikov et al. 1979). Therefore, $A/K \sim 1$ suggests the occurrence of hydroxyl radical-
112 based reaction pathways. In contrast, an A/K ratio different than 1 is indicative of a non-free
113 radical mechanism of oxidation, i.e., the presence of metal-based oxidant species (**Scheme**
114 **1b**). However, to our knowledge, Cy oxidation has never been used as a probe to clarify in a
115 systematic way the mechanism of the Fenton reactions in water.



116

117 **Scheme 1.** Proposed mechanism for cyclohexane oxidation. **A:** free radical path with Russel
118 termination type. **B:** a metal-based path.

119 By using this mechanistic tool based on Cy oxidation, in this work we develop a facile
120 method to provide evidence of the nature of Fenton reactive species in water in the presence
121 of several common Fe(II) ligands. Specifically, the A/K ratio is used as a selectivity proxy to
122 relate a structural parameter of the iron ligands (binding constants) with its influence on the
123 reaction. Furthermore, we demonstrate the possibility to control the reaction pathway by
124 adjusting the ligand concentration and other environmental conditions. One of the hypotheses
125 of this work is that numerous iron ligands can promote a metal-based reaction process. As
126 such, eight ligands are tested, namely, citric acid, tartaric acid, malic acid, quinic acid,
127 EDTA, EDDS, and NTA, as well as Fe-TAML[®] (see Figure S1 in the Supplementary
128 Material for its molecular structure). The first seven ligands are well-known iron chelators,
129 applied to perform oxidation reactions in water at near-neutral pH. Fe-TAML[®] and the classic
130 Fenton reagents (pH 3) are studied as standard controls for a metal-based and (supposed) free
131 radical process, respectively (Collins 2002; de Oliveira et al. 2007; Ghosh et al. 2008).
132 Through an active species linked to the iron-ligand complex, a metal-based mechanism can
133 modulate the path of the reaction and generate fewer and more predictable by-products.
134 Therefore, by verifying the involvement of a metal-based mechanism during a classic or
135 modified Fenton process in water, one can open the route toward a safer oxidation of
136 hazardous substances, e.g., phenols, pharmaceuticals, and pesticides.

137

138 **2. EXPERIMENTAL**

139 **2.1 Chemicals**

140 Fe(III)-TAML[®] was purchased from GreenOx Catalysts Inc. (Pittsburgh, PA, U.S.A.).

141 Sodium phosphate tribasic was obtained from Carlo Erba (Italy). All the other reagents,

142 buffer solutions, and solvents were purchased from Sigma-Aldrich. Water was of Milli-Q
143 quality (TOC 2 ppb, resistivity $\geq 18.2 \text{ M}\Omega \text{ cm}$).

144 **2.2 Reaction conditions**

145 The reaction experiments were carried out at room temperature in a 20 mL solution for 10
146 min under continuous stirring, and were performed within 40 mL vials equipped by caps
147 provided with septum. The concentrations of the catalyst (computed in terms of iron
148 concentration), reagent (hydrogen peroxide), and substrate (cyclohexane) were 10^{-7} , 10^{-6} ,
149 and 10^{-4} mol/L, respectively, resulting in a relative ratio of 1:10:1000. While a 1:10
150 catalyst:oxidant ratio is typical of engineered applications, an excess of substrate was used
151 here to avoid the subsequent oxidation of one of the major by-products, namely,
152 cyclohexanol. Phosphate buffer (10 mM) or perchloric acid were used to fix the pH. Because
153 the value of the solubility constant of phosphate with iron is approximately 10^{-16} , significant
154 formation of iron phosphate can be ruled out in favor of the formation of iron-ligand
155 complexes. All the reactions were quenched by using *tert*-butyl alcohol (t-BuOH) as
156 scavenger of reactive species (excess concentration of 30 mM, thus 300:1 compared to
157 cyclohexane) for subsequent analysis (Rahhal and Richter 1988; Farinelli et al. 2019). The
158 iron-ligand complexes were prepared in equimolar ratio in a concentrated stock solution (0.01
159 mM) by stirring the mixture of the iron and ligand for 5 min, and were then diluted to 0.1
160 μM .

161 **2.3 Analytical conditions**

162 The headspace, solid phase microextraction technique (HS-SPME) was chosen as extraction
163 method before carrying out GC-MS analysis. This technique does not require solvents and
164 allows for highly sensitive analyses. Following each reaction experiment, the vials were left
165 in a thermostatic bath at 50 °C for 10 min to promote the transfer of all the relevant

166 compounds into the gas-phase headspace. Then, a SPME fiber (df 75 μm , fiber assembly
167 carboxen/polydimethylsiloxane) was injected through the septum of the cap and was left in
168 the headspace for 10 min, before withdrawing it for the subsequent GC-MS analysis. Samples
169 were analyzed on an Agilent 6890 GC system coupled with an Agilent 5973N mass selective
170 detector (MSD). For the chromatographic separation, a Zebron-5MS capillary column (30
171 $\text{m} \cdot \times 250 \text{ mm} \cdot \times 0.25 \mu\text{m}$) was used. The injection port temperature was 280 $^{\circ}\text{C}$, and the oven
172 temperature program was set as follows: 40 $^{\circ}\text{C}$ for 5 min, then an increase to 310 $^{\circ}\text{C}$ at a rate
173 of 15 $^{\circ}\text{C}/\text{min}$ (total run time 28.00 min). Helium was used as carrier gas at a constant flow of
174 1.2 mL/min, and the injector was held in splitless mode. The interface temperature was
175 280 $^{\circ}\text{C}$, the ionization energy was 70 eV, and the mass spectrometer operated in SIM mode
176 acquiring the following fragments: 84, 56, 41 (cyclohexane); 82, 67, 57 (cyclohexanol); 98,
177 55, 42 (cyclohexanone). Duplicate experiments for some of the tests discussed in this study
178 indicated high repeatability of the results; the error associated to the data and presented below
179 is related to the intrinsic uncertainty of the SPME technique, computed as the average among
180 the standard deviations reported in the 525.2 method provided by the EPA.

181 A few control experiments were carried out to study the Fenton degradation of phenol (by
182 both $\text{Fe}^{2+} + \text{H}_2\text{O}_2$ and $\text{Fe}^{\text{III}}\text{-TAML}^{\text{®}} + \text{H}_2\text{O}_2$) using t-BuOH as scavenger, to take advantage of
183 the ability of this compound to react with $\bullet\text{OH}$ faster than with electron-capture oxidants,
184 such as ferryl (Buxton et al. 1988; Rahhal and Richter 1988). The time evolution of phenol
185 was monitored by liquid chromatography (see the Supplementary Material for additional
186 details).

187

188

189

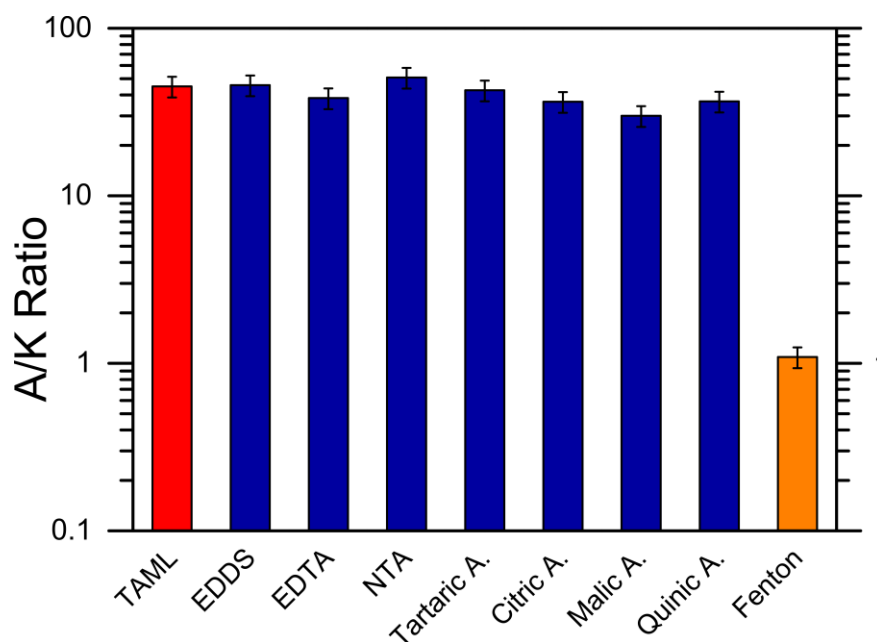
190

191 3. RESULTS AND DISCUSSION

192 3.1 Iron ligands promote the preferential formation of cyclohexanol

193 Eight widely available ligands able to complex iron in a stable fashion were tested, namely:
194 citric acid, tartaric acid, malic acid, quinic acid, EDTA (ethylenediaminetetraacetic acid),
195 EDDS (ethylenediamine-N,N'-disuccinic acid), NTA (nitrilotriacetate), and TAML
196 (tetraamidomacrocyclic ligand). These ligands belong to two macro-categories: natural
197 (citric, tartaric, malic, quinic acid) and artificial ligands (EDTA, EDDS, NTA, TAML). This
198 choice was provisionally made to gain insight into any possible correlation between the two
199 categories, or among ligands in the same category. The Fe-TAML[®] system is well-known to
200 induce a metal-based oxidation process via a ferryl species, thus we expected an
201 alcohol/ketone (A/K) product ratio different from 1 upon oxidation of cyclohexane (Collins
202 2002; de Oliveira et al. 2007). Conversely, the Fenton process at pH 3 generates mostly
203 hydroxyl radicals, or at least the hydroxyl radical is the most reactive (although not the only
204 one) species in the system. Therefore, the reaction should proceed mostly via a free radical
205 mechanism, with an A/K ratio around 1 (Minero et al. 2013).

206 **Figure 1** shows the A/K ratio values obtained with all the investigated ligands and in the
207 absence of ligands, i.e., classic Fenton. The results obtained from oxidation tests are in line
208 with expectations, thus attesting to the validity of the method. The classic Fenton process at
209 pH 3 showed an A/K ratio around 1, while an A/K ratio significantly higher than 1 was
210 obtained with all the other investigated ligands. Therefore, it is reasonable to hypothesize that
211 the presence of an iron ligand in water promotes a metal-based oxidation.



212
213

214 **Figure 1.** A/K ratio observed in the oxidation of cyclohexane with different iron ligands at
215 pH 7 (phosphate buffer) and with the classic Fenton process at pH 3 (perchloric acid) after 30
216 min of reaction.

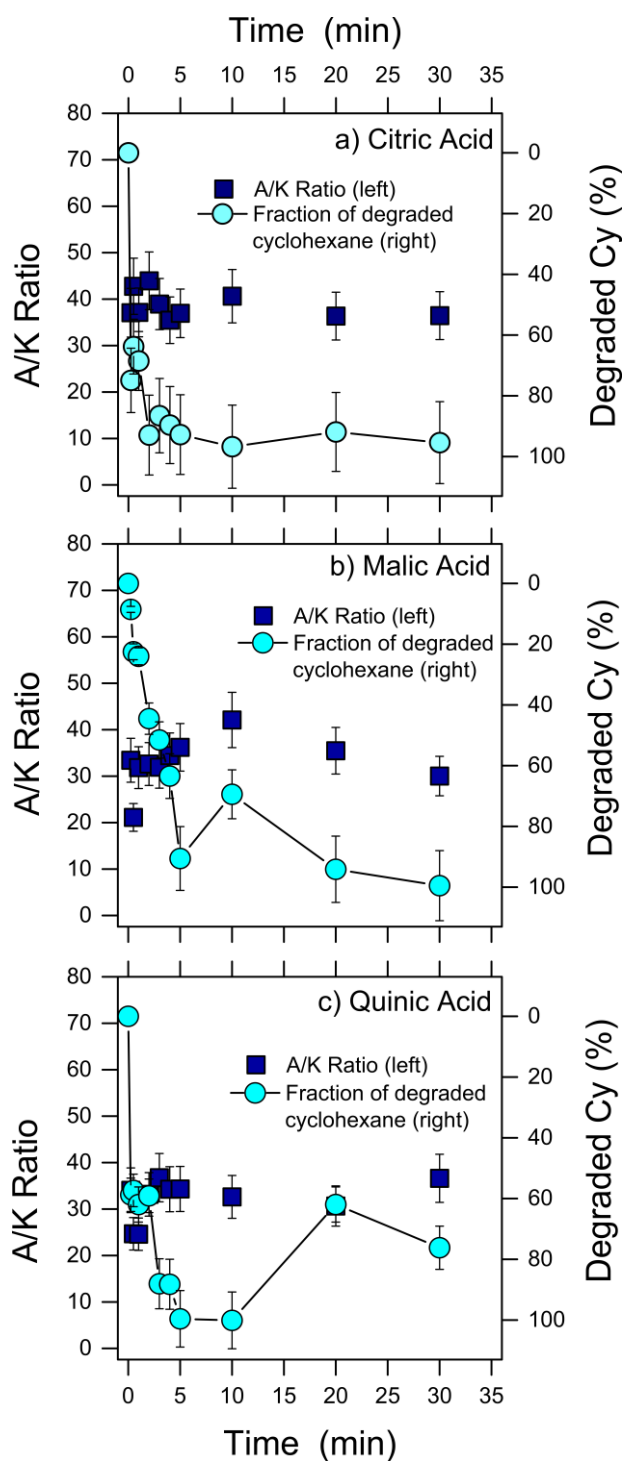
217

218 These conclusions are confirmed by the results of the degradation of phenol, with $\text{Fe}^{2+} +$
219 H_2O_2 at pH 3 and with $\text{Fe-TAML}^{\text{®}} + \text{H}_2\text{O}_2$ (see Figure S2 in Supplementary Material, as well
220 as the related text). We carried out these experiments both in the absence and in the presence
221 of t-BuOH, which reacts with $\bullet\text{OH}$ faster than with ferryl (Buxton et al. 1988; Rahhal and
222 Richter 1988). However, to avoid total quenching of the system by t-BuOH, the t-
223 BuOH:phenol ratio was 40:1 and not 300:1 as per the Cy experiments. In the case of $\text{Fe}^{2+} +$
224 H_2O_2 , t-BuOH strongly inhibited phenol degradation, while in the case of $\text{Fe-TAML}^{\text{®}}$ the
225 effect of the alcohol was practically negligible. These findings are consistent with $\bullet\text{OH}$ being
226 involved in phenol degradation by $\text{Fe}^{2+} + \text{H}_2\text{O}_2$ at pH 3, and with ferryl playing the same role
227 with $\text{Fe-TAML}^{\text{®}} + \text{H}_2\text{O}_2$. Indeed, the t-BuOH scavenging experiments agree with the A/K
228 ratios derived from the Cy degradation experiments (**Figure 1**).

229 It is important to check for possible variations of the A/K ratio with reaction time, to ensure
230 that unbiased conclusions are obtained. **Figure 2** shows the kinetics of Cy degradation with
231 citric acid (**Figure 2a**), malic acid (**Figure 2b**), and quinic acid (**Figure 2c**) as iron ligands
232 (left Y-axis: A/K ratio, right Y-axis: Cy degradation). Cy degradation with citric and quinic
233 acids was very fast and the process reached completion after roughly 2 min of reaction. The
234 corresponding A/K ratio remained stable and significantly larger than 1 during the entire
235 duration of the test (30 min). On the other hand, **Figure 2b** (malic acid) shows slower
236 kinetics of degradation, with an A/K ratio reaching a peak value after 10 min of reaction. This
237 slower degradation allowed for an easier monitoring of the initial preferred formation of the
238 alcohol species ($A/K > 1$) and the subsequent oxidation of the alcohol into the ketone, which
239 caused a slight A/K reduction following the peak. The large excess of the initial Cy
240 consumed almost all the reactive species, thereby limiting their availability for alcohol
241 oxidation. By monitoring the A/K time evolution, one can thus be confident that there is
242 negligible bias linked to the further evolution of the system ($A \rightarrow K$ oxidation, or further
243 Fenton processes involving, e.g., Fe(III) after total Fe(II) consumption) after the initial
244 reaction step (Russell 1957).

245 The fact that the A/K ratio did not change much after the initial step suggests that the
246 mechanistic conditions reflect those of the initial reaction between Fe(II) and H_2O_2 . Under
247 our experimental conditions and based on the stoichiometry of reaction (1), this process
248 would entail total consumption of Fe(II) that would be oxidized to Fe(III), and 10%
249 degradation of H_2O_2 . Afterwards, Fe(III) would be recycled to Fe(II) at the expense of the
250 remaining H_2O_2 .

251



252

253 **Figure 2.** Fraction of degraded cyclohexane with respect to the total degraded amount
 254 (circles, right axis) and trend of selectivity, i.e., A/K ratio (squares, left axis), as a function of
 255 time in a system containing hydrogen peroxide as reactant and a) citric acid, b) malic acid, or
 256 c) quinic acid as iron ligands. The pH of the aqueous system was buffered at 7 (phosphate
 257 buffer). The solid lines connecting the circles are only intended as a guide for the eye.

258 The influence of the reaction environment was also studied by following the A/K ratio in the
259 oxidation of Cy at different pH values (3-7) (**Table 1**). All the individual concentrations of
260 alcohol and ketone products obtained during the experiments are presented in the
261 Supplementary Material (Tables S1-S3). Citric, malic, and quinic acid were chosen as iron
262 ligands because the iron binding constant of these compounds would not change significantly
263 within the explored pH range, thereby allowing for the pH value to solely affect the Fenton
264 process (Supplementary Material, Figure S3). Phosphate (10 mM) was used to buffer the pH
265 at values of 5, 6, and 7, while perchloric acid (1.16 M stock solution) was employed in tests
266 performed at pH 3. In all these cases, the A/K ratios were higher than 1, independently of the
267 pH values. This finding suggests that a metal-based mechanism in the presence of the three
268 ligands was observed regardless of the acidity of the solution. Although acidity has no direct
269 effect on the mechanistic path, the conditional binding constant may be function of the pH
270 and this indirect effect of the solution acidity is discussed below.

271

272 **Table 1.** A/K ratio for the oxidation of cyclohexane at different pH values with citric, malic
273 and quinic acid as iron ligands. The pH was fixed with phosphate buffer except for pH 3
274 (HClO_4). The reaction time was 30 min.

275

	pH 3	pH 5	pH 6	pH 7
Citric acid	10±1	7.4±1.0	8.5±1.2	8.6±1.2
Malic acid	18±3	15±2	16±2	15±2
Quinic acid	28±4	31±4	23±3	28±4

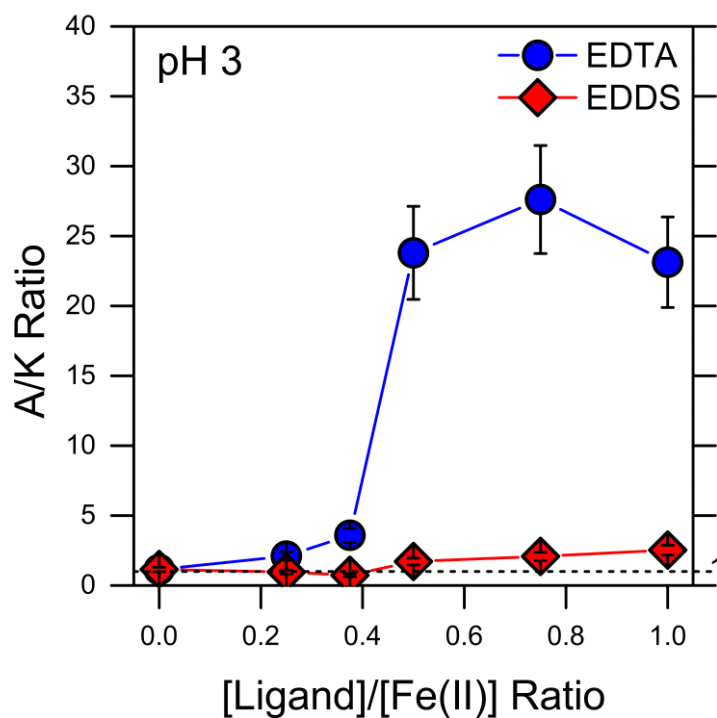
279

280 3.2 Switching the mechanism from free radical to metal-based catalysis

281 In the previous section, we hypothesized that the mechanistic degradation path depends on
282 the presence of the ligand, and possibly on its concentration and conditional binding constant.
283 In order to investigate the influence of the ligand concentration and of its conditional binding
284 constant with the metal (i.e., the value of the binding constant that takes into account the
285 protonation of the ligand at the given pH value), EDTA and EDDS were chosen as iron
286 ligands and applied at acidic pH. Despite their structural similarity, these two ligands behave
287 differently in terms of their conditional binding constant as a function of pH. Specifically,
288 while the conditional binding constant at pH 7 is high for both EDTA and EDDS ($\sim 10^{11}$ and
289 10^6 , respectively), at pH 3 EDDS features a low conditional binding constant (10^{-3}), while
290 that of EDTA is still relatively high ($\sim 10^4$) (see Supplementary Material, Figure S3).
291 Therefore, when using EDDS as iron ligand at pH 3, one expects a high amount of free iron
292 to occur in solution, which could reasonably induce a classic Fenton process (free radical
293 mechanism). In this series of experiments, the pH value was fixed at a value of 3 by addition
294 of perchloric acid.

295 **Figure 3** reports the A/K ratios observed when EDDS and EDTA were used as ligands at pH
296 3, at various [Ligand]:[Fe(II)] ratios. All the individual concentrations of alcohol and ketone
297 products obtained during the experiments are presented in the Supplementary Material
298 (Tables S4-S5). Please note that **Figure 1** summarized instead the A/K ratios measured at 1:1
299 [Ligand]:[Fe(II)] ratio and at pH 7. Consistently with the hypotheses, at 0:1 ligand:iron ratio
300 (i.e., with no ligand in solution) we observed the classic Fenton process and the A/K ratio
301 was close to 1. The A/K ratio remained always close to 1 with EDDS, regardless of its
302 concentration. Based on the conditional binding constants, when using EDDS as iron ligand
303 at pH 3, one expects free iron to occur in solution, which could reasonably promote a process
304 similar to a classic $\bullet\text{OH}$ -based Fenton reaction. In contrast, with EDTA the reaction clearly

305 switched from a free radical mechanism to a metal-based one when the ligand concentration
306 increased (Bernasconi and Baerends 2009; Mang et al. 2016). These results strongly suggest
307 that the presence of a bonded Fe(II)-ligand complex plays a crucial role in the direction of the
308 mechanistic path. This parameter is a strong function of the concentration of the ligand as
309 well as of the conditional binding constant of the complex metal/ligand. Therefore, one can
310 generalize that the mechanistic path may be mostly imputable to the concentration and to the
311 conditional binding constant of the ligand, and that the environmental conditions have
312 importance only if they affect complex formation.

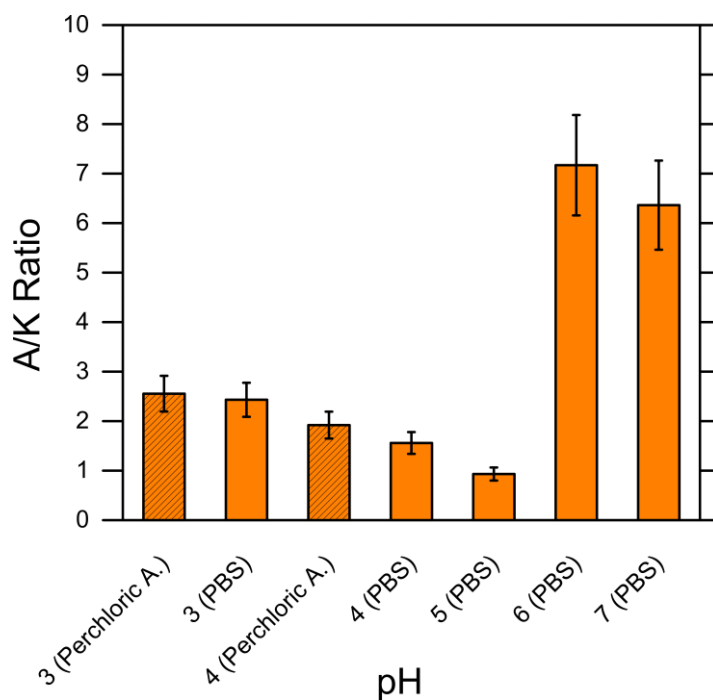


313
314 **Figure 3.** A/K ratio observed after 30 min of reaction in the oxidation of cyclohexane with
315 EDTA and EDDS as iron ligands, added at different concentrations. The runs were carried
316 out at pH 3. The condition of no added Ligand ($[\text{Ligand}]/[\text{Fe(II)}] = 0$) corresponds to the
317 classic Fenton process. The solid lines are only intended as a guide for the eye. The dashed
318 line depicts the expected A/K ratio for a pure free radicals-based catalysis.

319

320 3.3 Evidence of the effect of pH on the traditional Fenton process

321 Finally, we provide some insight into the Fenton mechanism at different pH values. **Figure 4**
322 shows the A/K ratio obtained with the classic Fenton process in the 3-7 pH range, fixed by
323 use of phosphate buffer (PBS). Additional experiments were also conducted by fixing the pH
324 at 3 and 4 using perchloric acid instead of phosphate buffer. Please note that Fe(II) was dosed
325 at low concentration (0.1 μM) to avoid its precipitation as hydroxide, which would otherwise
326 take place at near-neutral pH ($\text{pKs}^{\text{Fe(OH)}_2} = 15.1$ (Harris 2006)). The results obtained in the
327 absence of ligands imply that the classic Fenton reaction proceeds through a free radical or
328 mixed mechanism up to pH 5. Above this value, the mechanism switched to a preferential
329 metal-based one. This result is supported by previous reports proposing that a ferryl species is
330 involved in the Fenton reaction at near-neutral pH (Rush et al. 1990; Bossmann et al. 2004;
331 Bataineh et al. 2012). The presence of a ferryl species at pH 6-7 means that the classic Fenton
332 reaction will be less reactive under near-neutral conditions, since the non-coordinated ferryl
333 species is considered less reactive than the hydroxyl radical (Bataineh et al. 2012).



334

335 **Figure 4** A/K ratio observed in the classic Fenton process performed at different pH values.

336 4. CONCLUSIONS

337 The oxidation mechanism of the Fenton reaction was here investigated with and without iron
338 ligands in solution. Eight widely common ligands that are able to complex iron(II) were
339 studied, namely, citric acid, tartaric acid, malic acid, quinic acid, EDTA, EDDS, and NTA,
340 plus the Fe-TAML[®] system. The ligand performance was tested toward the oxidation of
341 cyclohexane by following the formation of the main products, namely, cyclohexanol (A) and
342 cyclohexanone (K). Measurement of the concentration ratio between these two species (A/K
343 ratio parameter) during the reaction provides evidence of the mechanism involved in the
344 oxidation of the substrate. This simple method was proven effective to discriminate in water
345 between the predominance of a non-selective active species, free radicals, or of a more
346 selective ferryl species.

347 All the tested ligands showed high A/K ratios, which is a proper index of a metal-based
348 behavior, including the well-known Fe-TAML[®] system that was expected to behave in this
349 fashion. Also expected was the fact that the classic Fenton process was associated with an
350 A/K ratio of approximately 1, evidence of a free radical process, which adds further evidence
351 in favor of cyclohexane as suitable probe when coupled with the A/K ratio. The results
352 suggested that the ligand/iron concentration ratio plays a role in the mechanism of reaction
353 and this parameter may be thus exploited to control the pathways of contaminant degradation
354 in water. Also, if the ligand-specific binding constant changes with environmental conditions,
355 e.g., the pH, the reaction mechanism may be controlled by adjusting such conditions.

356 This work proves the ability of simple iron ligands to drive the reaction pathway towards
357 selective metal-based catalysis. Selective catalysis allows for better control of the degradation
358 pathway of harmful contaminants, to avoid the formation of toxic by-products. The
359 ubiquitous character of the Fenton process in nature and of iron complexes formed in water

360 (e.g., citrate), alongside the generation of H₂O₂ in illuminated NOM-containing
361 environments, lead to (photo)Fenton reactions during the diurnal cycles. As such, the present
362 study holds important implications in the elucidation of the Fenton process that occurs both in
363 nature and in engineering applications, and represents a step further in understanding the
364 effectiveness of ligand-mediated oxidation of natural and anthropogenic contaminants.

365

366 **ASSOCIATED CONTENT**

367 **Supporting Information.** The Supporting Information is available free of charge on the ACS
368 Publications website

369 **AUTHOR INFORMATION**

370 **Corresponding Authors***

371 D.V.: Tel.: +39 0116705296. E-mail: davide.vione@unito.it

372 A.T.: Tel.: +39 0110907628. E-mail: alberto.tirafferri@polito.it

373 **Notes**

374 The authors declare no competing financial interest.

375

376 **ACKNOWLEDGMENTS**

377 This study was financially supported by Politecnico di Torino and University of Torino. D.V.
378 acknowledges financial support by University of Torino and Compagnia di San Paolo
379 (project CSTO168282-ABATEPHARM). S.G. acknowledges the Spanish Ministry of
380 Science, Innovation and Universities (MICIU) for the Ramón y Cajal Fellowship (RYC2018-
381 024033-I).

382

383 **References**

- 384 Barbeni, M., Minero, C., Pelizzetti, E., Borgarello, E., Serpone, N., 1987. Chemical
385 Degradation of Chlorophenols with Fenton Reagent (Fe-2++H₂O₂). *Chemosphere*. 16, 2225-
386 2237. [https://doi.org/10.1016/0045-6535\(87\)90281-5](https://doi.org/10.1016/0045-6535(87)90281-5)
- 387 Barbusinski, K., 2009. Fenton Reaction - Controversy Concerning the Chemistry. *Ecol.*
388 *Chem. Eng. S.* 16, 347-358.
- 389 Bataineh, H., Pestovsky, O., Bakac, A., 2012. pH-induced mechanistic changeover from
390 hydroxyl radicals to iron(IV) in the Fenton reaction. *Chem. Sci.* 3, 1594-1599.
391 <https://doi.org/10.1039/c2sc20099f>
- 392 Bernasconi, L., Baerends, E. J., 2009. Generation of Ferryl Species through Dioxygen
393 Activation in Iron/EDTA Systems: A Computational Study. *Inorg. Chem.* 48, 527-540.
394 <https://doi.org/10.1021/ic800998n>
- 395 Bossmann, S. H., Oliveros, E., Gob, S., Siegwart, S., Dahlen, E. P., Payawan, L., Straub, M.,
396 Worner, M., Braun, A. M., 1998. New evidence against hydroxyl radicals as reactive
397 intermediates in the thermal and photochemically enhanced fenton reactions. *J. Phys. Chem.*
398 *A.* 102, 5542-5550. <https://doi.org/10.1021/Jp980129j>
- 399 Bossmann, S. H., Oliveros, E., Kantor, M., Niebler, S., Bonfill, A., Shahin, N., Worner, M.,
400 Braun, A. M., 2004. New insights into the mechanisms of the thermal Fenton reactions
401 occurring using different iron(II)-complexes. *Water Sci. Technol.* 49, 75-80.
402 <https://doi.org/10.2166/wst.2004.0224>
- 403 Buxton, G. V., Greenstock, C. L., Helman, W. P., Ross, A. B., 1988. Critical-Review of Rate
404 Constants for Reactions of Hydrated Electrons, Hydrogen-Atoms and Hydroxyl Radicals
405 (.Oh/.O-) in Aqueous-Solution. *J. Phys. Chem. Ref. Data.* 17, 513-886. <https://doi.org/Doi>
406 10.1063/1.555805
- 407 Clarizia, L., Russo, D., Di Somma, I., Marotta, R., Andreozzi, R., 2017. Homogeneous
408 photo-Fenton processes at near neutral pH: A review. *Appl. Catal. B-Environ.* 209, 358-371.
409 <https://doi.org/10.1016/j.apcatb.2017.03.011>
- 410 Collins, T. J., 2002. TAML oxidant activators: A new approach to the activation of hydrogen
411 peroxide for environmentally significant problems. *Acc. Chem. Res.* 35, 782-790.
412 <https://doi.org/10.1021/ar010079s>
- 413 Das, B., Baruah, J. B., Sharma, M., Sarma, B., Varunak, G. V., Satyanarayana, L., Roy, S.,
414 Bhattacharyya, P. K., Kanta Borah, K., Bania, K. K., 2020. Self pH regulated iron(II) catalyst
415 for radical free oxidation of benzyl alcohols. *Appl. Catal. A-Gen.* 589, 117292.
416 <https://doi.org/10.1016/j.apcata.2019.117292>
- 417 de Oliveira, F. T., Chanda, A., Banerjee, D., Shan, X. P., Mondal, S., Que, L., Bominaar, E.
418 L., Munck, E., Collins, T. J., 2007. Chemical and spectroscopic evidence for an Fe-V-Oxo
419 complex. *Science.* 315, 835-838. <https://doi.org/10.1126/science.1133417>

420 Dong, J. J., Fernandez-Fueyo, E., Hollmann, F., Paul, C. E., Pesic, M., Schmidt, S., Wang, Y.
421 H., Younes, S., Zhang, W. Y., 2018. Biocatalytic Oxidation Reactions: A Chemist's
422 Perspective. *Angew. Chem. Int. Edit.* 57, 9238-9261. <https://doi.org/10.1002/anie.201800343>

423 dos Santos, J. S., Palaretti, V., de Faria, A. L., Crevelin, E. J., de Moraes, L. A. B., Assis, M.
424 D., 2011. Biomimetic simazine oxidation catalyzed by metalloporphyrins. *Appl. Catal. A-*
425 *Gen.* 408, 163-170. <https://doi.org/10.1016/j.apcata.2011.09.023>

426 England, J., Davies, C. R., Banaru, M., White, A. J. P., Britovsek, G. J. P., 2008. Catalyst
427 stability determines the catalytic activity of non-heme iron catalysts in the oxidation of
428 alkanes. *Adv. Synth. Catal.* 350, 883-897. <https://doi.org/10.1002/adsc.200700462>

429 Farinelli, G., Minella, M., Sordello, F., Vione, D., Tiraferri, A., 2019. Metabisulfite as an
430 Unconventional Reagent for Green Oxidation of Emerging Contaminants Using an Iron-
431 Based Catalyst. *Acs Omega.* 4, 20732-20741. <https://doi.org/10.1021/acsomega.9b03088>

432 Fenton, H. G. H., 1894. LXXIII.—Oxidation of tartaric acid in presence of iron *J. Chem. Soc.*
433 *Trans.* 65, 899-910. <https://doi.org/10.1039/CT8946500899>

434 Ghosh, A., Mitchell, D. A., Chanda, A., Ryabov, A. D., Popescu, D. L., Upham, E. C.,
435 Collins, G. J., Collins, T. J., 2008. Catalase-Peroxidase Activity of Iron(III)-TAML
436 Activators of Hydrogen Peroxide. *J. Am. Chem. Soc.* 130, 15116-15126.
437 <https://doi.org/10.1021/ja8043689>

438 Giannakis, S., 2019. A review of the concepts, recent advances and niche applications of the
439 (photo) Fenton process, beyond water/wastewater treatment: Surface functionalization,
440 biomass treatment, combatting cancer and other medical uses. *Appl. Catal. B-Environ.* 248,
441 309-319. <https://doi.org/10.1016/j.apcatb.2019.02.025>

442 Giannakis, S., Ruales-Lonfat, C., Rtimi, S., Thabet, S., Cotton, P., Pulgarin, C., 2016. Castles
443 fall from inside: Evidence for dominant internal photo-catalytic mechanisms during treatment
444 of *Saccharomyces cerevisiae* by photo-Fenton at near-neutral pH. *Appl. Catal. B-Environ.*
445 185, 150-162. <https://doi.org/10.1016/j.apcatb.2015.12.016>

446 Goldstein, S., Meyerstein, D., Czapski, G., 1993. The Fenton Reagents. *Free Radic. Biol.*
447 *Med.* 15, 435-445. [https://doi.org/10.1016/0891-5849\(93\)90043-T](https://doi.org/10.1016/0891-5849(93)90043-T)

448 Haber, F., Weiss, J., 1932. On the catalysis of hydroperoxide. *Naturwissenschaften.* 20, 948-
449 950. <https://doi.org/10.1007/BF01504715>

450 Harris, D. (2006). Quantitative Chemical Analysis, W. H. Freeman.

451 Hohenberger, J., Ray, K., Meyer, K., 2012. The biology and chemistry of high-valent iron-
452 oxo and iron-nitrido complexes. *Nat. Commun.* 3, <https://doi.org/10.1038/Ncomms1718>

453 Iwahashi, H., Ishii, T., Sugata, R., Kido, R., 1990. The Effects of Caffeic Acid and Its
454 Related Catechols on Hydroxyl Radical Formation by 3-Hydroxyanthranilic Acid, Ferric-
455 Chloride, and Hydrogen-Peroxide. *Arch. Biochem. Biophys.* 276, 242-247.
456 [https://doi.org/10.1016/0003-9861\(90\)90033-U](https://doi.org/10.1016/0003-9861(90)90033-U)

457 Klopstra, M., Roelfes, G., Hage, R., Kellogg, R. M., Feringa, B. L., 2004. Non-heme iron
458 complexes for stereoselective oxidation: Tuning of the selectivity in dihydroxylation using
459 different solvents. *Eur. J. Inorg. Chem.* 846-856. <https://doi.org/10.1002/ejic.200300667>

460 Lipczynskakochany, E., 1991. Degradation of Aqueous Nitrophenols and Nitrobenzene by
461 Means of the Fenton Reaction. *Chemosphere.* 22, 529-536. [https://doi.org/10.1016/0045-](https://doi.org/10.1016/0045-6535(91)90064-K)
462 [6535\(91\)90064-K](https://doi.org/10.1016/0045-6535(91)90064-K)

463 Liu, X. C., Zhou, Y. Y., Zhang, J. C., Luo, L., Yang, Y., Huang, H. L., Peng, H., Tang, L.,
464 Mu, Y., 2018. Insight into electro-Fenton and photo-Fenton for the degradation of antibiotics:
465 Mechanism study and research gaps. *Chem. Eng. J.* 347, 379-397.
466 <https://doi.org/10.1016/j.cej.2018.04.142>

467 Maillard, C., Guillard, C., Pichat, P., 1992. Comparative Effects of the Tio₂-Uv, H₂O₂-Uv,
468 H₂O₂-Fe²⁺ Systems on the Disappearance Rate of Benzamide and 4-Hydroxybenzamide in
469 Water. *Chemosphere.* 24, 1085-1094. [https://doi.org/Doi 10.1016/0045-6535\(92\)90199-2](https://doi.org/Doi 10.1016/0045-6535(92)90199-2)

470 Mang, Y., Klammerth, N., Messele, S. A., Chelme-Ayala, P., El-Din, M. G., 2016. Kinetics
471 study on the degradation of a model naphthenic acid by ethylenediamine-N,N'-disuccinic
472 acid-modified Fenton process. *J. Hazard. Mater.* 318, 371-378.
473 <https://doi.org/10.1016/j.jhazmat.2016.06.063>

474 Meslennikov, S. I., Galimova, L. G., Komissarov, V. D., 1979. Disproportionation Rate and
475 Products of Cyclohexylperoxy Radicals. *B. Acad. Sci. Ussr Ch+.* 28, 585-588.
476 <https://doi.org/10.1007/Bf00924841>

477 Messele, S. A., Bengoa, C., Stuber, F. E., Giralt, J., Fortuny, A., Fabregat, A., Font, J., 2019.
478 Enhanced Degradation of Phenol by a Fenton-Like System (Fe/EDTA/H₂O₂) at
479 Circumneutral pH. *Catalysts.* 9, 474. <https://doi.org/10.3390/Catal9050474>

480 Minero, C., Lucchiari, M., Maurino, V., Vione, D., 2013. A quantitative assessment of the
481 production of (OH)-O-center dot and additional oxidants in the dark Fenton reaction: Fenton
482 degradation of aromatic amines. *RSC Adv.* 3, 26443-26450.
483 <https://doi.org/10.1039/c3ra44585b>

484 Oloo, W. N., Que, L. (2013). Hydrocarbon Oxidations Catalyzed by Bio-Inspired Nonheme
485 Iron and Copper Catalyst. *Comprehensive Inorganic Chemistry II*, Elsevier.

486 Pan, Y., Zhou, M. H., Wang, Q., Cai, J. J., Tian, Y. S., Zhang, Y., 2020. EDTA, oxalate, and
487 phosphate ions enhanced reactive oxygen species generation and sulfamethazine removal by
488 zero-valent iron. *J. Hazard. Mater.* 391, 122210.
489 <https://doi.org/10.1016/j.jhazmat.2020.122210>

490 Park, J. S. B., Wood, P. M., Davies, M. J., Gilbert, B. C., Whitwood, A. C., 1997. A kinetic
491 and ESR investigation of Iron(II) oxalate oxidation by hydrogen peroxide and dioxygen as a
492 source of hydroxyl radicals. *Free Radic. Res.* 27, 447-458.
493 <https://doi.org/10.3109/10715769709065785>

494 Pignatello, J. J., Liu, D., Huston, P., 1999. Evidence for an additional oxidant in the
495 photoassisted Fenton reaction. *Environ. Sci. Technol.* 33, 1832-1839.
496 <https://doi.org/10.1021/Es980969b>

497 Rahhal, S., Richter, H. W., 1988. Reduction of Hydrogen-Peroxide by the Ferrous Iron
498 Chelate of Diethylenetriamine-N,N,N',N'',N''-Pentaacetate. *J. Am. Chem. Soc.* 110, 3126-
499 3133. <https://doi.org/10.1021/Ja00218a022>

500 Ricceri, F., Giagnorio, M., Farinelli, G., Blandini, G., Minella, M., Vione, D., Tiraferri, A.,
501 2019. Desalination of Produced Water by Membrane Distillation: Effect of the Feed
502 Components and of a Pre-treatment by Fenton Oxidation. *Sci. Rep.* 9,
503 <https://doi.org/10.1038/S41598-019-51167-Z>

504 Rush, J. D., Koppenol, W. H., 1986. Oxidizing Intermediates in the Reaction of Ferrous Edta
505 with Hydrogen Peroxide - Reactions with Organic-Molecules and Ferrocyclochrome-C. *J.*
506 *Biol. Chem.* 261, 6730-6733.

507 Rush, J. D., Koppenol, W. H., 1988. Reactions of Fe(II) and Fe(III) with Hydrogen-
508 Peroxide. *J. Am. Chem. Soc.* 110, 4957-4963. <https://doi.org/10.1021/Ja00223a013>

509 Rush, J. D., Maskos, Z., Koppenol, W. H., 1990. Distinction between Hydroxyl Radical and
510 Ferryl Species. *Method. Enzymol.* 186, 148-156. [https://doi.org/10.1016/0076-
511 6879\(90\)86104-4](https://doi.org/10.1016/0076-6879(90)86104-4)

512 Russell, G., A., 1957. Deuterium-isotope Effects in the Autoxidation of Alkyl
513 Hydrocarbons. Mechanism of the Interaction of Peroxy Radicals. *J. Am. Chem. Soc.* 79,
514 3871-3877. <https://doi.org/10.1021/ja01571a068>

515 Song, Q., Ma, W. H., Jia, M. K., Johnson, D., Huang, Y. P., 2015. Degradation of organic
516 pollutants in waters by a water-insoluble iron(III) Schiff base complex. *Appl. Catal. A-Gen.*
517 505, 70-76. <https://doi.org/10.1016/j.apcata.2015.07.028>

518 Southworth, B. A., Voelker, B. M., 2003. Hydroxyl radical production via the photo-Fenton
519 reaction in the presence of fulvic acid. *Environ. Sci. Technol.* 37, 1130-1136.
520 <https://doi.org/10.1021/es020757l>

521 Sutton, H. C., Vile, G. F., Winterbourn, C. C., 1987. Radical Driven Fenton Reactions -
522 Evidence from Paraquat Radical Studies for Production of Tetravalent Iron in the Presence
523 and Absence of Ethylenediaminetetraacetic Acid. *Arch. Biochem. Biophys.* 256, 462-471.
524 [https://doi.org/10.1016/0003-9861\(87\)90603-5](https://doi.org/10.1016/0003-9861(87)90603-5)

525 Vione, D., Minella, M., Maurino, V., Minero, C., 2014. Indirect Photochemistry in Sunlit
526 Surface Waters: Photoinduced Production of Reactive Transient Species. *Chem.-Eur. J.* 20,
527 10590-10606. <https://doi.org/10.1002/chem.201400413>

528 Wink, D. A., Nims, R. W., Saavedra, J. E., Utermahlen, W. E., Ford, P. C., 1994. The Fenton
529 Oxidation Mechanism - Reactivities of Biologically Relevant Substrates with 2 Oxidizing
530 Intermediates Differ from Those Predicted for the Hydroxyl Radical. *Proc. Natl. Acad. Sci.*
531 91, 6604-6608. <https://doi.org/10.1073/pnas.91.14.6604>

532 Yamazaki, I., Piette, L. H., 1990. ESR Spin-Trapping Studies on the Reaction of Fe²⁺ Ions
533 with H₂O₂-Reactive Species in Oxygen-Toxicity in Biology. *J. Biol. Chem.* 265, 13589-
534 13594.

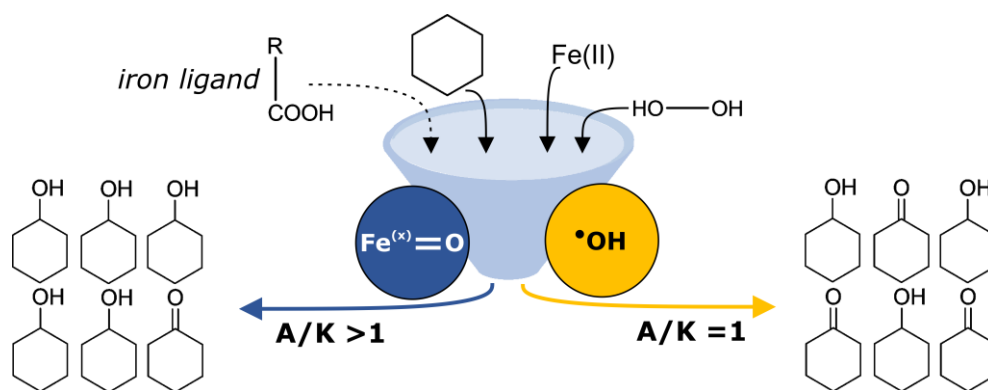
535 Zhang, H., Zhang, D. B., Zhou, J. Y., 2006. Removal of COD from landfill leachate by
536 electro-Fenton method. J. Hazard. Mater. 135, 106-111.
537 <https://doi.org/10.1016/j.jhazmat.2005.11.025>

538 Zhang, Y., Zhou, M. H., 2019. A critical review of the application of chelating agents to
539 enable Fenton and 1 Fenton-like reactions at high pH values. J. Hazard. Mater. 362, 436-450.
540 <https://doi.org/10.1016/j.jhazmat.2018.09.035>

541

542

543 **Graphical Abstract**



544

545